

BOUNDARY LAYER RESPONSE TO TRAVELLING SURFACE WAVES AT HIGH REYNOLDS NUMBER

I. Fumarola*, M. Santer and J. F. Morrison

Department of Aeronautics
Imperial College London
Exhibition Road, SW7 2AZ London
isabella.fumarola12@imperial.ac.uk

ABSTRACT

Numerical and experimental studies have demonstrated that skin friction drag can be reduced by a moving wall. Different types of motion, such as wall spanwise oscillation or spanwise waves travelling in the streamwise direction, have been investigated achieving greater than 40% skin friction drag reduction. Nevertheless, many open questions still remain on how surface waves interact with the turbulent boundary layer, in particular at high Reynolds number. In this paper, a 1 m² active surface is investigated at Re_τ between 4500 and 9000. The surface is able to generate well defined spanwise waves at different frequencies and wavelengths thanks to a deformable skin mounted on a kagome lattice mechanism driven by pneumatic actuators. This work analyses preliminary results of the flow response to different wavelengths and flow conditions. The boundary layer profiles are measured using a single hot-wire anemometer. The surface deformation is fully characterised using Stereo Digital Image Correlation (DIC) measurements over a large area of actuation. The model is shown to generate well defined in-plane travelling waves of spanwise velocity at the desired frequency and wavelength. Four different regimes have been tested, all showing a very similar flow response. A clear effect to the inner layer is observed, although no evident skin friction drag reduction is found. This work is the first experimental campaign of a high challenging experimental model, which will bring new insight into the interaction between spanwise travelling waves and turbulent boundary layer.

INTRODUCTION

In the context of climate change and air pollution and with the air traffic growing at a fast pace, there is an urgent need to find new technological solutions to reduce drag on planes. Several flow control mechanism, active and passive, have been proposed for skin friction drag reduction, since that counts for over 40% of the total drag in cruise conditions. Among them, one of the most promising active flow control mechanism is moving wall in the spanwise directions. Different type of wall motion have been considered by numerical simulations, leading to the most promising waves of spanwise velocity travelling in the streamwise direction:

$$W(x, 0, z, t) = W_0 \cdot \sin(1/\lambda_x x - 2\pi f t) \quad (1)$$

where x and z are the streamwise and spanwise directions respectively, λ_x the wavelength, f the frequency and W_0 the

speed amplitude.

In particular, it has been shown that waves travelling in the direction opposite to the flow can interact with the turbulent structures close to the wall leading up to 40% of skin friction drag reduction at $Re_\tau = 200$ Ricco *et al.* (2021). On the other hand, numerical simulations at higher Reynolds, up to $Re_\tau = 2000$, have shown that the amount of drag reduction should decrease with increased Reynolds, see Ricco *et al.* (2021). This result leads to the open question on the effectiveness of the mechanism at even higher Reynolds number, closer to flight conditions, at which numerical simulations become very challenging.

The problem has been recently addressed by Rouhi *et al.* (2023) and Chandran *et al.* (2023), who proposed a new path for drag reduction which aims to target the drag generated by the outer scales (Outer Scale Actuation, OSA) rather than the inner scales only (Inner Scale Actuation, ISA). The idea lies in the fact that the contribution of the outer scales to the total skin friction drag becomes more important at higher Reynolds number and by interacting with those structure the actuation frequency can be kept relatively low, therefore the mechanism would have the potential of producing drag reduction in more energy efficient way. Following this concept, the authors achieved 26% of skin friction drag reduction in a LES simulation at $Re_\tau = 4000$ and equivalent in a wind tunnel experimental campaign at Re_τ between 4500 and 16000.

As of today, that is the only work that has investigated spanwise surface wave at high Re_τ . Systematic experiments are therefore required to reveal the details of the fundamental mechanisms.

The difficult of high Reynolds number experiments depends on the boundary layer (δ) which becomes thinner if the speed is increased. To overcome this challenge the present experiment has been designed for the 10x5 wind tunnel at Imperial College London, which is characterised by a test section long 20 m. In this way, the Re_τ of the boundary layer is achieved by increasing the development length, maintaining a relatively low speed. As consequence, also the actuation frequency can be kept relatively low.

As far as the active surface concerned these are two main challenges. The first is related to the active surface size, which times by at least 3 boundary layer thickness in the spanwise direction to achieve flow uniformity and it needs to be long enough in the streamwise direction to obtained an equilibrium boundary layer which has adapted to the the new boundary conditions. The second challenge lies on the ability to generate in-plane, well-defined, sinusoidal waves which

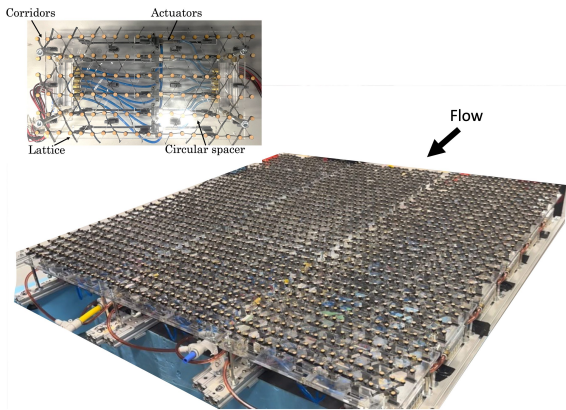


Figure 1: Active surface without silicone skin. In the top right corner a detail view of an individual module.

resemble the boundary conditions of the numerical simulation, equation 1. In previous studies (Chandran *et al.*, 2023) the wave was produced by rectangular slats moving relative to each other, which, make a spatially discretised wave. In this work, we present results from a first experimental campaign on an 1 m² active surface based on a kagome lattice, which as explained in the following section, is able to generate well-defined sinusoidal waves. The model is tested for several wave parameters at $4500 \leq Re_\tau \leq 9000$.

THE MODEL

The model comprises a flat plate, with a modified super-elliptic leading edge, resting on the floor of the wind tunnel. An active surface is installed 14 m downstream of the leading edge and it extends about 1 m both in streamwise and in spanwise direction, figure 1 and 2. The spanwise length is 1 meter, which is equivalent to about three times the boundary layer thickness to guarantee spanwise homogeneity in the flow.

The active surface consists of a pre-tensioned continuous black silicone skin glued to 18 *modules* of kagome lattice, arranged by 3 spanwise rows of 6 modules each, figure 1. Each module, as shown in the top left corner of figure 1, consists of 6 spanwise corridors. Each corridor is connected to a push/pull pneumatic actuator whose movement deforms the lattice non linearly, in a controlled and repeatable manner. Individual actuators are controlled by two solenoid valves, making a total of 216 digital outputs connected to a NI PXI system operated through a LabVIEW code. Details of the mechanical design of a lattice can be found in Bird *et al.* (2018).

The surface is able to generate spanwise travelling waves with different wave parameters, where the minimum wavelength is 55.4 mm and the range of frequencies is 5 Hz to 40 Hz. The main advantage of this mechanism, compared to others proposed in literature, are that it generates well-defined sinusoidal waves both in space and time and that frequency and wavelength can be varied independently.

THE EXPERIMENT

The experiment has been conducted in the 10x5 wind tunnel which has a test section of 3 m x 1.5 m for a length of

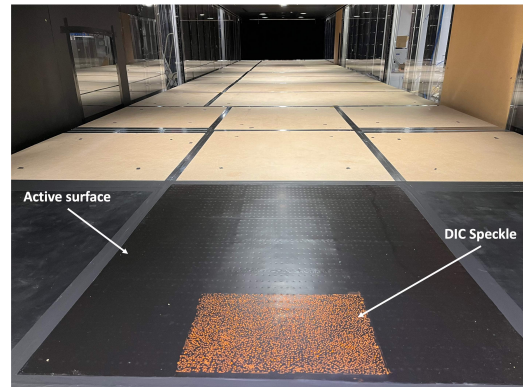


Figure 2: Model mounted in the wind tunnel with the orange DIC speckle visible on the surface.

20 m and a turbulence intensity of 0.15%.

To characterise the boundary layer response to the actuation, a hot wire has been aligned close to the wall just behind the last actuators and traversed in the wall-normal direction away from the surface. At each location without and with actuation to minimise the uncertainty on the distance from the wall. Each point is acquired at 60 kHz, using a lowpass filter at 30 kHz for 60 s. This corresponds to a large eddy turnover time of about $tU_\infty/\delta \approx 1500$.

The experimental setup includes three high speed cameras mounted on the roof of the wind tunnel to carry out simultaneous measurements of surface deformation and flow field using respectively planar Particle Image Velocimetry (PIV) and stereo Digital Image Correlation (DIC). PIV and DIC are both based on the correlation of image pairs. PIV captures the motion of the seeding particles in a narrow area illuminated by a laser sheet, while DIC the motion of random dots painted on the surface illuminated by a diffuse light that generates a speckle pattern. The implementation of PIV and DIC together for wind tunnel experiments is a relatively new approach for fluid-structure interaction problems. In a previous study, the two techniques have been combined using a three-colour scheme, where a the fluorescent speckle was illuminated by a blue LED and a green laser was used for the PIV, see Fumarola *et al.* (2023). The present experiment is the first to exploit the two techniques using only one light source, the PIV laser. This not only provides a compact setup but also guarantees simultaneous measurement. That is possible since the PIV laser sheet is in a streamwise-spanwise plane at a constant distance of 3.5 mm above the surface (corresponding to $39 \leq y^+ \leq 92$ depending on the freestream speed), which is enough to excite the speckle pattern. The speckle is painted using an orange fluorescent paint which emits at wavelengths around 650 nm when excited by the green laser at 527 nm. The background of the surface is painted matt black to enhance the contrast in the DIC images and to guarantee a similar level of darkness between the speckle and the background on the PIV camera. The cameras are equipped with filters to enable the PIV camera to record only light reflected by the seeding particles (green) and the DIC cameras to record only light emitted by the speckle pattern (orange). Images are acquired at a sampling rate of 500 Hz. Double frame mode is used for PIV while single frame for DIC. To improve the brightness of the speckle, the DIC camera is exposed during both PIV frames, that is possible since the surface does not move in the DIC image during that interval. An example of the combined

Test	U_∞ (m/s)	u_τ (m/s)	Re_τ	f (Hz)	λ (mm)	ω^+	T^+	k^+	W^+
A	6.68	0.23	4570	10	55.4	4.54E-04	350	0.0074	0.5
B	7.75	0.27	5360	10	55.4	3.30E-04	483	0.0063	0.4
C	9.60	0.32	6360	10	55.4	2.35E-04	678	0.005	0.3
D	10.65	0.34	6850	10	110.8	2.02E-04	788	0.0024	0.3

Table 1: Flow and surface conditions for each test case.

results is shown in figure 4, but only results from the DIC are discussed in this paper.

Four different cases of upstream travelling waves are investigated. The freestream speed is varied between 7 m/s and 10 m/s, which corresponds to Re_τ between ≈ 4500 and ≈ 9000 at the measurement location. The actuator frequency is kept at 10 Hz, while the wavelength is varied between 55.4 mm and 110.8 mm, as reported in table 1. All the cases tested here had the actuation frequency in the OSA regime since $T^+ > 350$ (Rouhi *et al.*, 2023). The operational parameters were chosen to be in the most promising area of drag reduction by the proposed large scale mechanism according to the LES by Rouhi *et al.* (2023), as shown in in figure 3.

RESULTS

For any active flow control mechanism it is important to fully characterise the input to the flow, which is the motion of the active surface. To this scope the Stereo DIC measurements provide a well defined 3D time-resolved deformation field over an of 380 mm x 240 mm, which corresponds to 9 rows of actuator. An example of the surface deformation in the case D in table 1 is reported in figure 5 and figure 6.

Figure 5 shows an example of the time series of the displacements in the three directions of one point of the surface: streamwise D_x , wall-normal D_y , spanwise D_z , with corresponding Fourier transform. Clearly the maximum displacement is in the spanwise direction, which is characterised by an approximate sinusoidal wave at 10 Hz, figure 5e and 5f. For the nature of the lattice's deformation, the spanwise displacement is always associated with a small deformation in the streamwise direction. Finally, the wall normal displacement is less than ± 0.5 mm.

The spanwise velocity at the wall, W_0 , is calculated from the time resolved displacement as reported in figures 6a. The surface speed as function of time appears to be a well defined sinusoid at the desired frequency. Having obtained a velocity deformation in time and space, it is possible to calculate the double power spectra density of the surface speed $M_{W_0}^+$, as shown in figure 6b. The figures have been expressed in non dimensional units, using the skin friction velocity obtained from the hot-wire results for the non actuated surface as explained below. The contour plot of the surface speed confirms that most of the energy is concentrated at the desired actuation frequency and wavelength, as indicated by the dashed line in figure and reported in table 1. The effectiveness of the mechanism has been verified also for the surface parameters of the other tests.

In terms of flow field response to the actuation, the hot-wire profiles for all the cases show a similar trend. For brevity, only the hot-wire boundary layer profile for the two higher Re_τ , cases C and D in table 1, are presented in figure 7. The

boundary layer has been non dimensionalised based on the non actuated skin friction velocity, $u_{\tau,0}$, which is calculated using the Clauser method. The actuated mean velocity appeared shifted to higher velocities in the inner layer. This would suggest an increase in the skin friction velocity, although the friction velocity results unchanged if the Clauser method is used. A clear effect in the inner layer appears also in the variance of the velocity. The maximum point of fluctuation is shifted towards the wall and increases its value for the actuated case. The pre-multiplied spectra, figure 8, reveals that the increase in energy close to the surface is related to the actuation frequency but also to its in the range of 100 Hz, which corresponds to $T^+ = 100$. Whether that is an actual effect of the flow or is due to an influence of the actuators to the hot-wire signal is still under investigation. Oil film interferometry measurements will be implemented to obtain a direct, independent, measurement of the skin friction in the next experimental campaign.

CONCLUSIONS

In this work, a new active surface model to study drag reduction due to surface wave at high Reynolds number is presented. Results from a first experimental campaign have been presented. The measurements from the DIC demonstrate the ability of the surface to generate well-defined spanwise waves travelling at the desired frequency and wavelength. The results from the hot-wire are somewhat unexpected, but consistent between all the cases tested, as they would indicate a drag increase instead of drag reduction. To this end a future experimental campaign will aim to validate the results using oil film interferometry to directly measure the skin friction at a location immediately downstream of the active surface. Further work also includes the manufacturing of two more tiles of active surface which will be aligned in the streamwise direction to cover a total area of 3 m x 1 m, which will correspond to 9 boundary layer thickness in streamwise and 3 in spanwise. This will enable measurements on a fully developed turbulent boundary layer completely adjusted to the new surface conditions.

Acknowledgments

This work has been funded by EPSRC Grant no. EP/R032467/1.

REFERENCES

- Bird, James, Santer, Matthew & Morrison, Jonathan F 2018 Experimental control of turbulent boundary layers with in-plane travelling waves. *Flow, turbulence and combustion* **100**, 1015–1035.

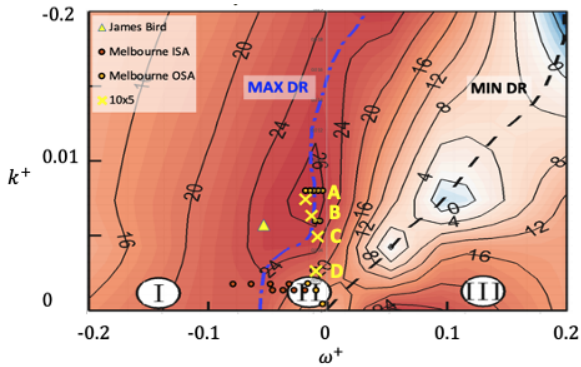


Figure 3: Experimental parameters superimposed to drag reduction map as function of k^+ and ω^+ at Re_τ 4000, adaptation from numerical simulation in Rouhi *et al.* (2023).

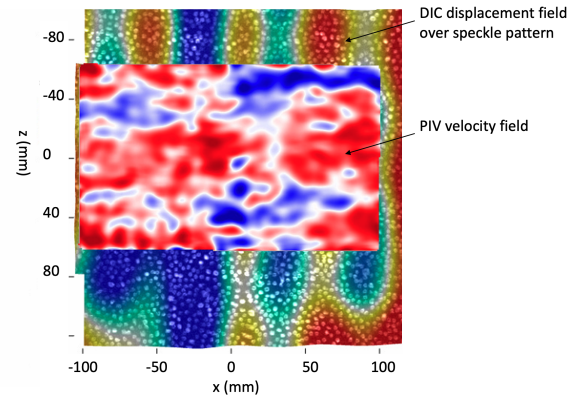


Figure 4: Example of PIV results superimposed on the displacement field from the DIC for a surface wave at $f = 10$ Hz and $\lambda = 55.4$ mm. The colour map of the DIC represents the spanwise displacement, blue corresponds to negative and red to positive spanwise displacement. The flow is left to right.

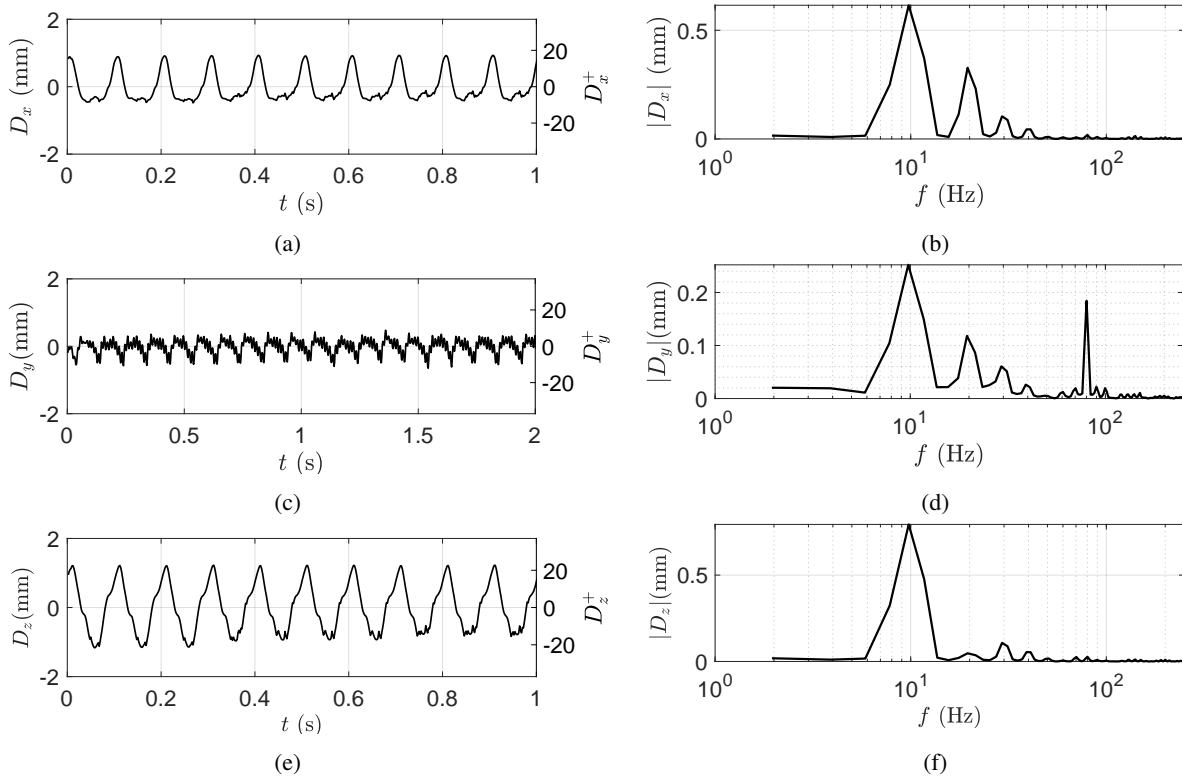


Figure 5: Example of time series of the surface displacement in the streamwise, wall-normal and spanwise direction from the DIC measurement and corresponding spectra.

Chandran, D., Zampiron, A., Rouhi, A., Fu, M.K., Wine, D., Holloway, B., Smits, A.J. & Marusic, I. 2023 Turbulent drag reduction by spanwise wall forcing. part 2. high-reynolds-number experiments. *Journal of Fluid Mechanics* **968**, A7.
 Fumarola, I., Santer, M. & Morrison, J. 2023 Simultaneous

measurements of surface spanwise waves and velocity in a turbulent boundary layer, (under revision). *Flow, turbulence and combustion*.

Ricco, Pierre, Skote, Martin & Leschziner, Michael A. 2021 A review of turbulent skin-friction drag reduction by near-wall

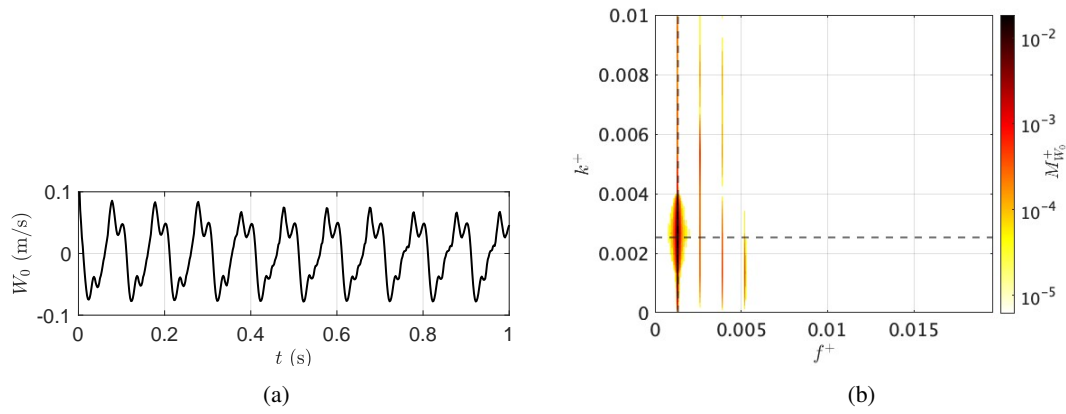


Figure 6: Surface speed measured by the DIC cameras: a) example of time series from one point of the surface; b) double spectra of the surface speed, as function of frequency and wavenumber for the travelling wave of case D in table 1. The dashed lines indicate the desired actuated frequency and wavenumber. The data has been non-dimensionalised using the $u_{\tau,0}$ from the non actuated case.

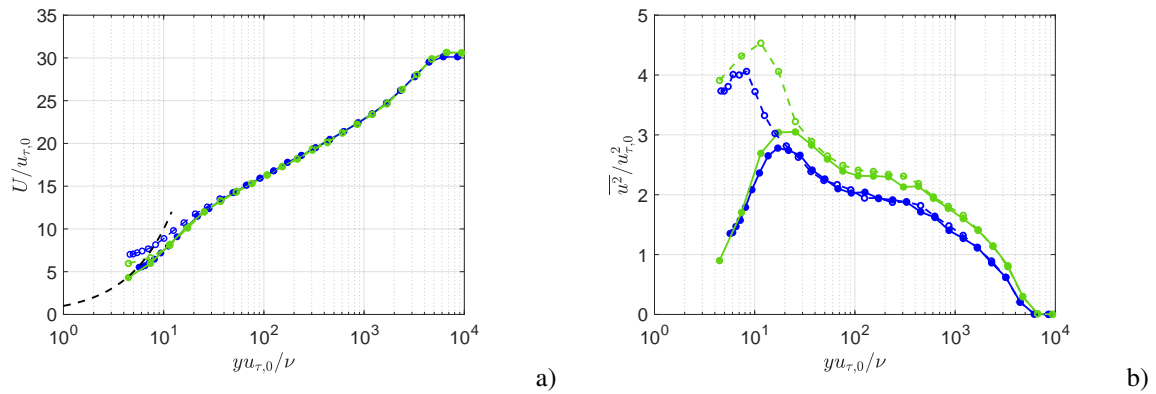


Figure 7: Velocity profile without actuation (full dots, continuous line) and with actuation (empty dots, dashed line) at Re_{τ} 6000 for case C, at $f = 10$ Hz for $\lambda = 55.4$ mm, (blue) and case D, at $\lambda = 110.8$ mm, (green).

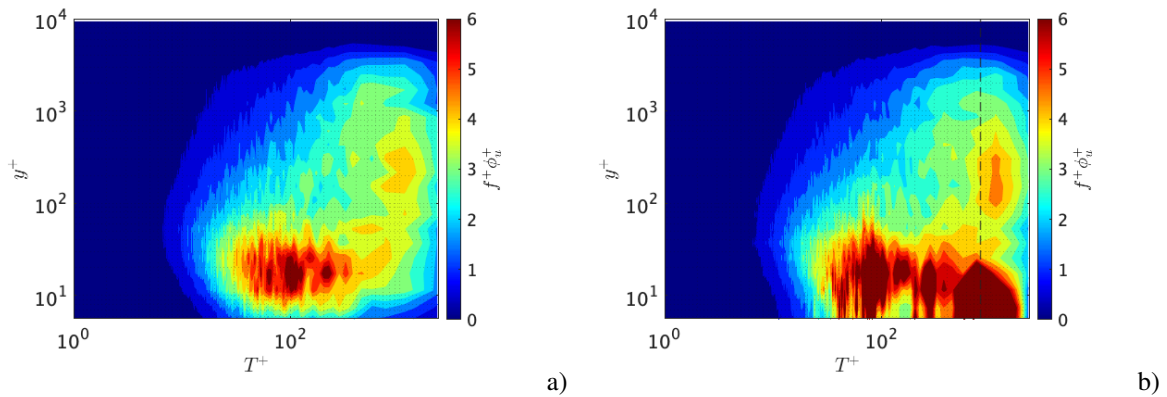


Figure 8: Pre-multiplied spectra a) without actuation and b) with actuation for the case D in table 1. The dashed line represents the actuation frequency.

transverse forcing. *Progress in Aerospace Sciences* **123**, 100713.

Rouhi, Amirreza, Fu, Matt K, Chandran, Dileep, Zampiron, Andrea, Smits, Alexander J & Marusic, Ivan 2023

Turbulent drag reduction by spanwise wall forcing. part 1. large-eddy simulations. *Journal of Fluid Mechanics* **968**, A6.